Fatigue Load Spectra for a Steel Girder Bridge

ANDRZEJ S. NOWAK, HANI NASSIF, AND KARL H. FRANK

The objective is to present an approach for the evaluation of fatigue performance. The proposed method is a combination analytical and experimental approach. The steps include identification of critical components and details, determination of the load distribution factors and stress range, instrumentation of the bridge, measurement of strains under a control vehicle to calibrate the equipment and determine the load distribution factors, measurement of strain under normal traffic, verification of load distribution factors, verification of load range, and evaluation of fatigue performance. Critical components and details are identified on the basis of analysis and past experience. The analysis provides theoretical values of load distribution factors and stress ranges. Measurement results provide a basis for verification of the analytical values. The number of load cycles is determined from the stress record under normal traffic. For a given number of load cycles, the effective stress range is calculated and compared with the critical level. Then the remaining fatigue life is estimated as a percent of the remaining number of cycles to failure. This serves as a basis for the evaluation of fatigue performance. The proposed approach is applied to an existing steel girder bridge. The superstructure consists of four plate girders and transverse floor beams. The bridge is instrumented, and the results of measurements are presented and discussed. For the considered components and details, the measured stress range and estimated number of load cycles are not critical. Some minor cracking may be expected, but in general the bridge may be considered as adequate with regard to fatigue.

Knowledge of fatigue load spectra is important in evaluating the performance of existing steel bridges. Live load effects may be different for different components and details. In many cases analytical methods do not allow for an accurate estimation of load, in particular load distribution factor and actual stress range. Therefore there is a need for field measurements to verify the analytical results.

Estimation of fatigue life of an existing bridge involves evaluation of fatigue resistance (capacity) and load spectra. Fatigue resistance depends on material properties, type of detail, degree of corrosion, and other deterioration. Load analysis requires knowledge of load history (accumulated damage), current load spectra, and prediction of future loads. The objective of this paper is to present an approach to evaluation of the fatigue load for an existing steel girder bridge.

The load is modeled on the basis of weigh-in-motion (WIM) measurements, truck count, and statistical analysis. The resulting load spectrum (number of cycles and effective stress range) is compared with fatigue strength. This comparison serves as a basis for evaluation of the adequacy of the considered component or detail.

The approach is demonstrated on the evaluation of fatigue performance for the Woodrow Wilson Memorial Bridge (*1*). The structure carries Interstate I-95 over the Potomac River between Maryland and Virginia. When the bridge was opened to traffic in 1962, the average daily traffic (ADT) was estimated to be 75,000. The current ADT is 165,000, and it is estimated that it will increase in the future to 235,000. There are three lanes of traffic in each direction. The bridge has a moveable portion, which is not considered in this study.

EVALUATION PROCEDURE

The procedure for evaluating fatigue performance includes analysis and field measurements. A list of the major steps follows.

1. Review the available drawings. Identify the fatigue-prone components and details on the basis of experience. Special attention should be paid to distortion-induced fatigue (transverse components and connections, varying stiffness of girders).
2. Perform analysis to determine the load spectra for main girders (load distribution factors) and fatigue-prone components and details.
3. Instrument the bridge and take WIM measurements. Measure the actual load distribution to girders (girder distribution factors). Measure stress and stress range under a normal flow of traffic.
4. Verify the accuracy of analytical girder distribution factors by comparison with measured distribution factors.
5. Verify the calculated stress ranges by comparison with measured values.
6. Establish the cumulative distribution functions for stress range (for the critical components and details).
7. Estimate the fatigue resistance of the critical components and details.
8. Evaluate the fatigue performance of critical components and details by comparison of load and resistance.
9. Estimate the remaining fatigue life.

The evaluation of fatigue load (Steps 3–6) is the primary consideration here. The instrumentation and measurements are described for the bridge. The formula for the remaining fatigue life, in terms of number of load cycles to failure, is also provided.

A. S. Nowak and H. Nassif, Department of Civil and Environmental Engineering, 2370 CG Brown Building, University of Michigan, Ann Arbor, Mich. 48109. K. H. Frank, Department of Civil Engineering, University of Texas, Austin, Tex. 78712.

INSTRUMENTATION

The tests were performed on the western approach spans, shown in Figure 1. The bridge, considered the Woodrow Wilson Memorial Bridge, is a multispan continuous structure with typical spans equal to 19 m (62 ft). The superstructure consists of four steel plate girders spaced at 7.8 m (25 ft 8 in.), as shown in Figure 2. Main girders have identical webs; however flanges are larger in interior girders. Therefore exterior girders have a lower stiffness than interior girders. Transverse floor beams are spaced at 6.3 m (20 ft 8 in.). The calculations showed high fatigue stress levels in exterior girders. To verify the analytical results, strain gauges were installed at these locations. Evaluation of plans and site inspection revealed other fatigue-prone details. Several years ago cracks were observed in the connections of transverse floor beams with main girders. Another fatigue-prone detail was intersection of longitudinal to transverse stiffener. Typical connection and stiffeners of floor beam to girder are shown in Figure 3.

The bridge was instrumented using strain gauges and strain gauge transducers. In particular, strains were measured at the critical connections between floor beams and exterior girders. Main girders were instrumented to verify girder distribution factors. The location of strain gauges is shown in Figure 4. A test truck was used to determine bridge response to a known load and to compare the measured response to that obtained by analysis. The test truck was a three-axle vehicle with a total weight of 275 kN (62.5 kips).

The waveform of the measured stresses agreed with the predictions, an indication that the bridge was responding as predicted in the analysis. However the measured stresses were always considerably less than the calculated stresses, because of the distribution of the truck load to the adjacent girders in the actual bridge.

Examples of typical plots of the floor beam gauge outputs are shown in Figure 5. The recorded stress ranges resulting from the test truck are presented in Tables 1 and 2, for the truck in the right and center lanes, respectively. On average the response for the truck in the center lane was 50 percent larger than the response for the truck in the right lane.

The floor beam gauges produced some unexpected results. The stresses measured at the end of the floor beams, near the exterior girder, indicate that the top flange of the floor beam is subjected to compression and that the bottom flange is subjected to tension during passage of the test truck over the floor beam. It was expected that the stresses would have the opposite sign. If the floor beam behaves as a fixed-end beam, loaded in the center, with no rotation and displacement at its ends, the stress would have been tension at top and compression on the bottom at the connection to the exterior girder. The measured compression stress at the top and tension stress at the bottom of the floor beam at its exterior

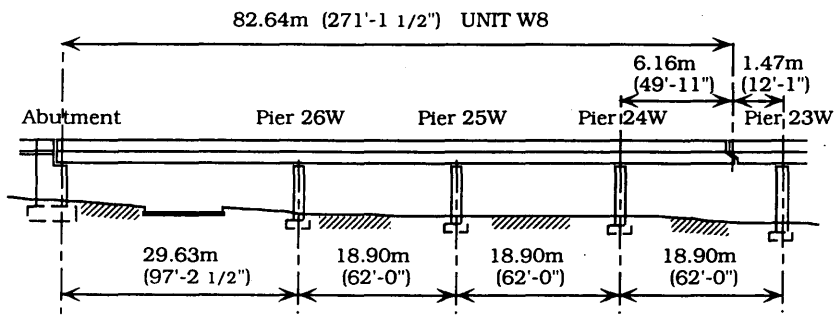

FIGURE 1 Elevation of considered portion of bridge.

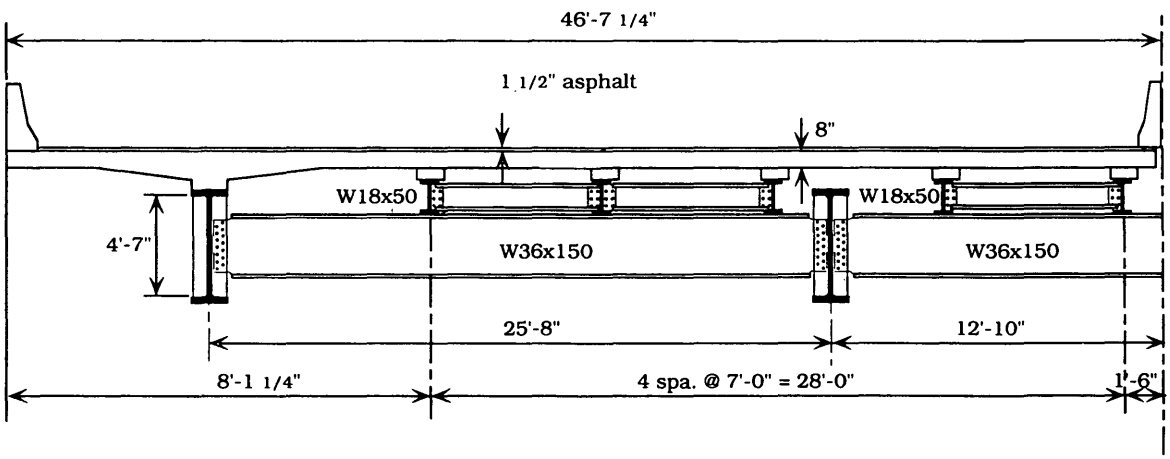

FIGURE 2 Cross section of bridge.

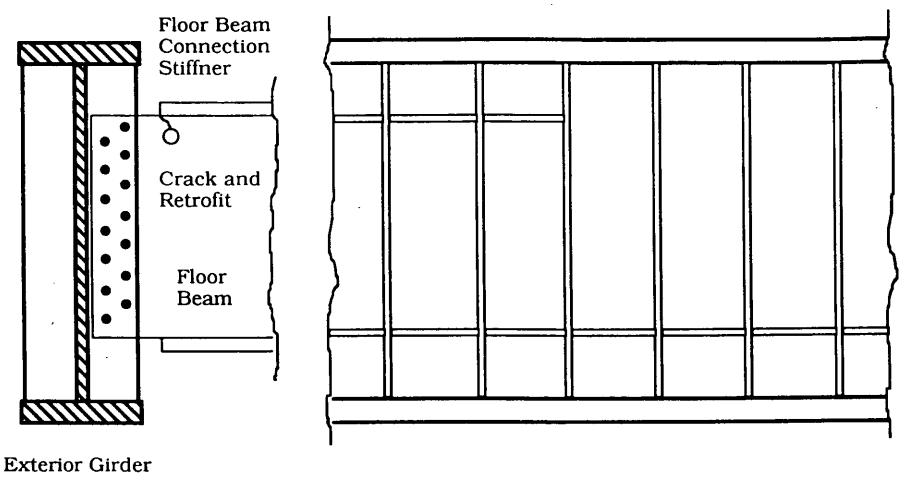

FIGURE 3 Girder-to-floor beam connection and stiffener intersection.

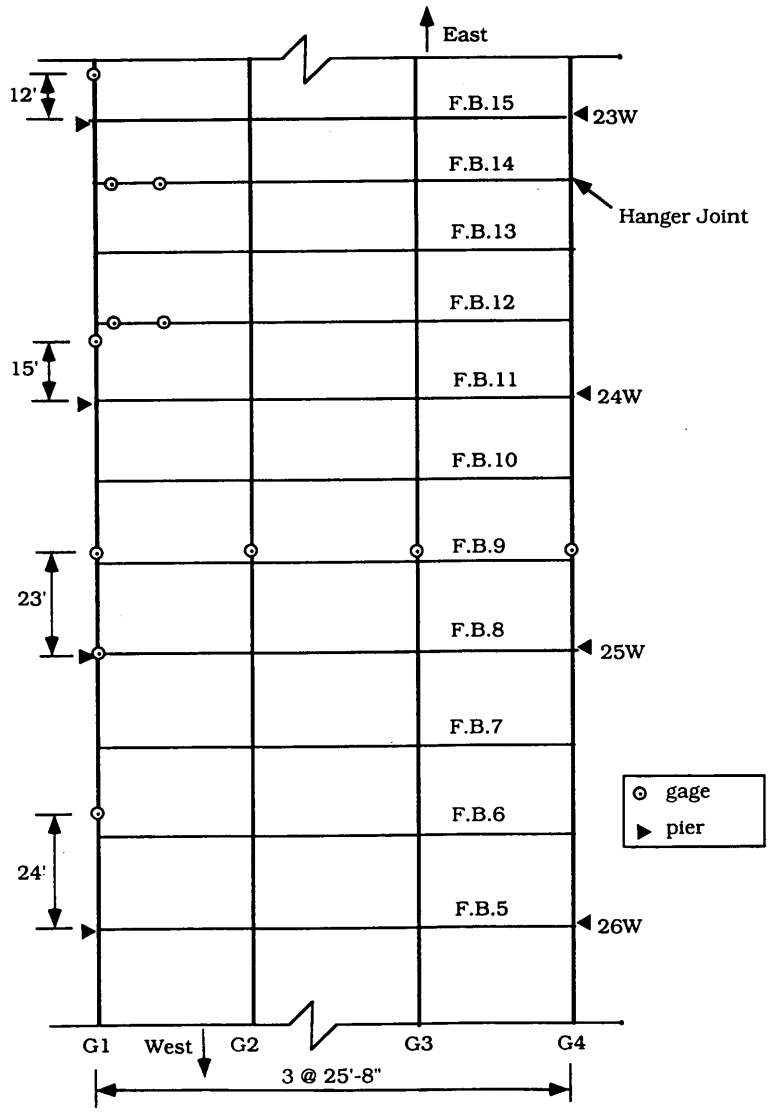

FIGURE 4 Location of strain gauges.

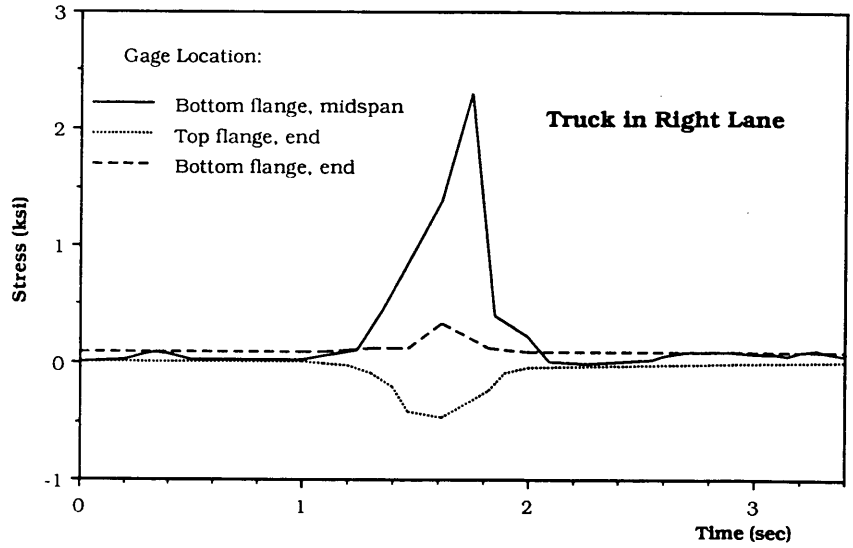

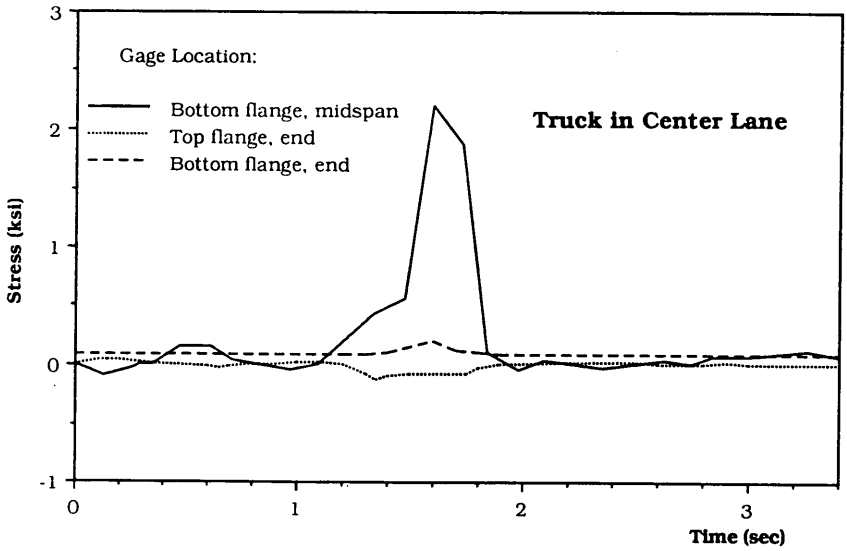

FIGURE 5 Typical stress range versus time for floor beam.

TABLE 1 Stress Ranges for Test Truck in Right Lane

Gage location Number of girder	Distance from support	Top/bottom	Stress Range (ksi) Measured	Calculated	Measured/ Calculated
First week:					
G1	24'	bottom	2.43	9.24	.263
G1	12'	bottom	3.49	9.98	.350
G1	0'	top	0.51	4.93	.104
G1	15'	bottom	1.16	6.87	.169
Second week:					
G2	5'	bottom	1.01	6.18	.163
G1	9.5'	bottom	4.00	9.61	.416

1' = 305 mm; 1 ksi = 6.89 MPa

TABLE 2 Stress Ranges for Test Truck in Center Lane

Gage location			Stress Range (ksi)		Measured/
Number of girder	Distance from support	Top/bottom	Measured	Calculated	Calculated
First week:					
G1	24'	bottom	1.15	9.24	.124
G1	12'	bottom	1.59	9.98	.159
G1	0'	top	0.25	4.93	.051
G1	15'	bottom	0.44	6.87	.064
Second week:					
G2	5'	bottom	1.70	6.18	.275
G1	9.5'	bottom	1.76	9.61	.183

1' = 305 mm; 1 ksi = 6.89 MPa

support indicate that it is responding as a beam fixed against rotation but undergoing a relative displacement between its supports, the exterior, and the first interior girders. The primary stresses at the end of the floor beams are generated by the differential deflection of the girders and not by the fixed-end moments caused by the rotational restraint provided by the girders. The floor beams are acting like a cantilever from the interior girders supporting the more flexible exterior girders.

To determine the lateral distribution of truck load, gauges were placed at the bottom flanges at the midspans of the main girders. The resulting stress ranges are shown in Figure 6. Each curve corresponds to a passage of the test truck. The highest stress ranges were observed in exterior girders for the controlled truck traveling in the right lanes, close to the exterior girders. The lateral distribution of the moment caused by the truck weight is shown in Figure 7. In Figure 7, a mo-

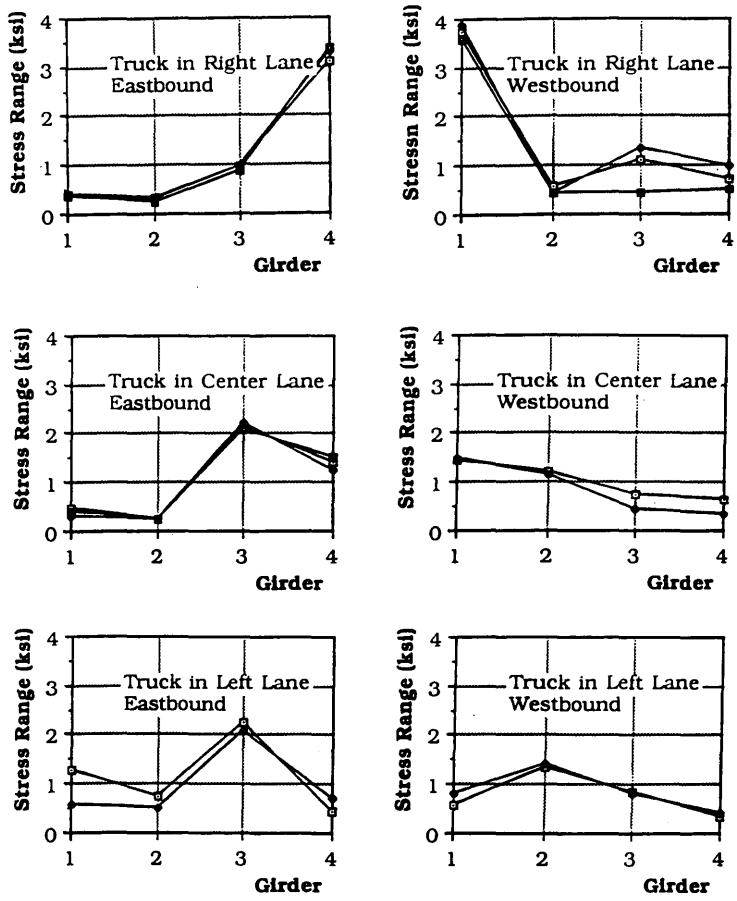

FIGURE 6 Measured stress in girders for various truck positions.

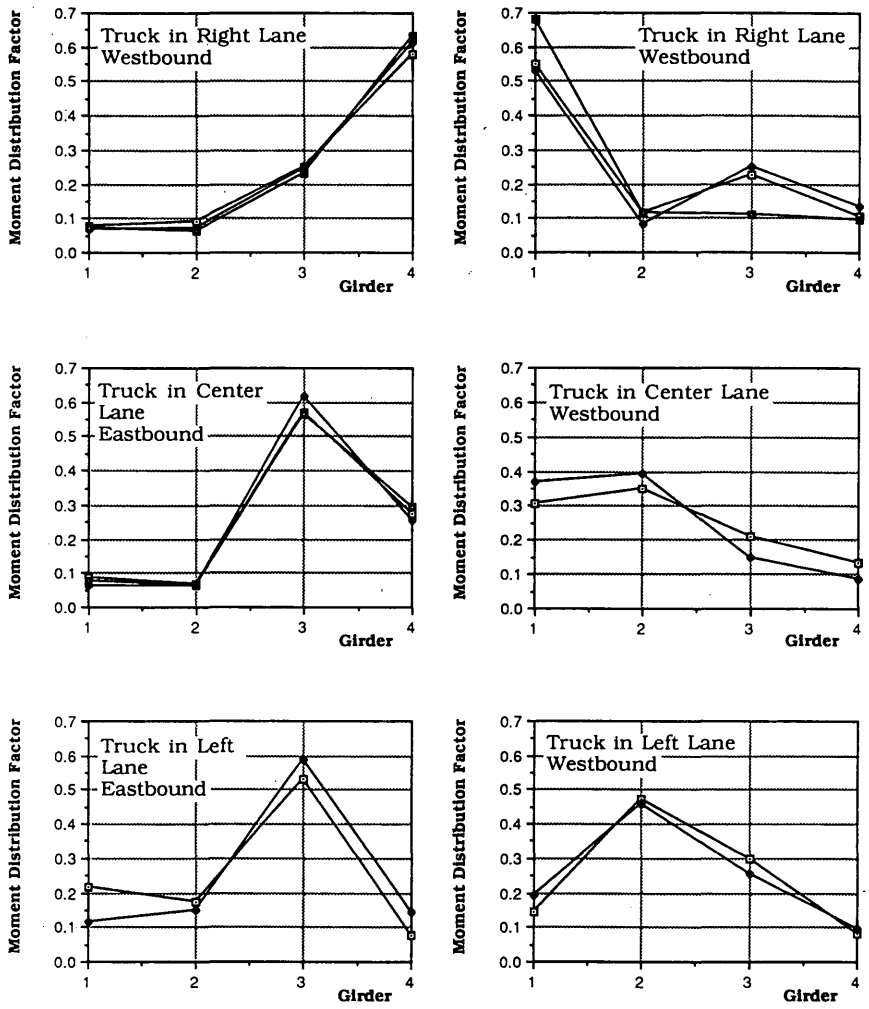

FIGURE 7 Moment distribution to girders.

ment distribution factor denotes the fraction of the total moment resisted by a girder.

TRUCK SURVEY

To verify the estimates of truck numbers, the Maryland Department of Transportation (DOT) carried out a traffic survey. The traffic flow was recorded for 24 hr with a video camera. The filmed traffic was analyzed to count trucks in each lane and direction. Multiple presence cases (more than one truck per span) were also counted. A total of 11,334 trucks was counted, with 5,174 in the eastbound direction. Less than 10 percent of trucks used the left lane (closest to the median). Approximately every 20th to 25th truck is on the bridge simultaneously with another truck moving side by side in the adjacent lane (within the same span and traveling in the same direction).

The number of trucks also was obtained from the strain/stress data in field tests. The measurements were carried out continuously for 2 weeks. The equipment counts the stress cycles at each location using a rainflow counting scheme. The rainflow counting method counts each individual stress cycle measured. The fatigue life estimate is based on Miner's rule, which includes all the measured stress cycles. The number of stress ranges at various levels is stored for each day counted.

In the fatigue analysis, the average daily truck traffic (ADTT) values are based on the results of truck surveys, field tests, and Maryland DOT estimates. They vary from 7,000 in 1962 (opening of the bridge) to 12,000 in 1991 to an estimated 16,000 in 2010.

NORMAL TRAFFIC TESTS

The girder gauges and floor beam gauges were installed to measure the stresses caused by normal traffic on the bridge. Results are plotted in a histogram of the stress range at each location as well as an effective stress range calculation. A typical histogram of the stress range is shown in Figure 8. The effective stress range, S_{ref}, is the stress range of constant amplitude that would produce the same fatigue damage as the variable amplitude stresses recorded on the bridge. It can be determined from the linear damage assumption (*2,3*) as

$$S_{ref} = \sqrt[3]{\Sigma(S_i^3 \gamma_i)} \quad (1)$$

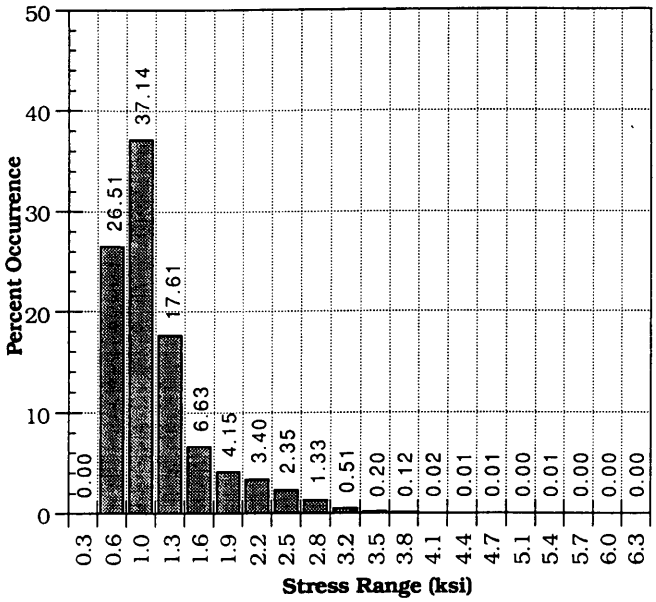

FIGURE 8 Typical histogram of stress range.

where

$$\gamma_i = n_i/n \quad (2)$$

where n_i is the number of cycles recorded at stress level S_i and n is the total number of stress cycles recorded.

The effective stress range and the number of cycles counted were used to evaluate the expected fatigue performance of the bridge. The largest traffic volume was observed on Wednesday; therefore Wednesday traffic was used as a reference. The results of measurements and calculations are presented in Table 3. Girders are denoted by G1 (exterior girder) and G2 (interior girder). Floor beams are denoted by FB. Strain gauges were attached to bottom or top flange of girders and floor beams. Location of a strain gauge is described by the distance from the support (pier). The number of cycles recorded on each Wednesday and the effective stress range of each gauge are given. The sixth column presents the number of cycles measured at the gauge divided by the estimated ADTT of 12,000 both ways from the truck traffic prediction. The number of cycles at each gauge is different because of the counting threshold imposed. In the first test week stress ranges below 3.5 MPa (0.5 ksi) were ignored. In the second week the level was reduced to 1.75 MPa (0.25 ksi). It was observed that about half the westbound trucks produced a measured stress cycle. The readings for floor beams indicate that each truck had two axles that produced a stress cycle.

TABLE 3 Effective Stress Range and Number of Cycles

Gage No.	location: Distance	Top/ bottom	Stress Cycles Wednesday	S_{ref} (ksi)	Cycles/ 12,000
First week:					
G1	24'	bottom	6,679	1.12	0.56
G1	12'	bottom	5,746	1.39	0.48
G1	0'	top	33	0.70	0.00
G1	15'	bottom	450	0.77	0.04
FB	midspan	bottom	7,062	1.28	0.59
FB	midspan	bottom	7,103	1.29	0.59
Second week:					
G2	5'	bottom	5,906	1.07	0.49
G1	9.5'	bottom	6,560	1.49	0.55
FB	midspan	bottom	11,794	1.01	0.98
FB	midspan	bottom	12,387	1.03	1.03

1' = 305 mm; 1 ksi = 6.89 MPa

FATIGUE LOAD ANALYSIS

The fatigue life of a welded detail, expressed in terms of the number of load cycles (N) may be represented as

$$N = A/S_{ref}^3 \quad (3)$$

where A is a constant depending on the welded detail and S_{ref} is the effective stress range. The value of A may be calculated from the values of stress range and life (number of load cycles) in the AASHTO specification (1989) for each category of welded detail. The fraction of the fatigue life consumed for the given number of cycles, n, and effective stress range, S_{ref}, is denoted by D and may be calculated as

$$D = n\,S_{ref}^3/A \quad (4)$$

Using the estimated past, present, and future ADTT, the percent of the fatigue life of the girders and floor beams were estimated. The estimated life is calculated for AASHTO Category C, D, E, and E′ details. The stiffener intersection fatigue category was also evaluated. Fatigue life was estimated for the weld at the end of a longitudinal stiffener close to a transverse stiffener weld. This is a severe fatigue detail producing lives below a Category E′ (denoted by > E′). The fraction of fatigue life consumed, D, is plotted versus year in Figures 9, 10, and 11, for a girder, floor beam, and stiffener intersection, respectively. For girders and floor beams, the value of D is determined for detail categories C, D, E, E′ and >E′. For a stiffener intersection, only category >E′ is considered. The analysis based on experimental results indicates that only the stiffener intersection detail has a potential

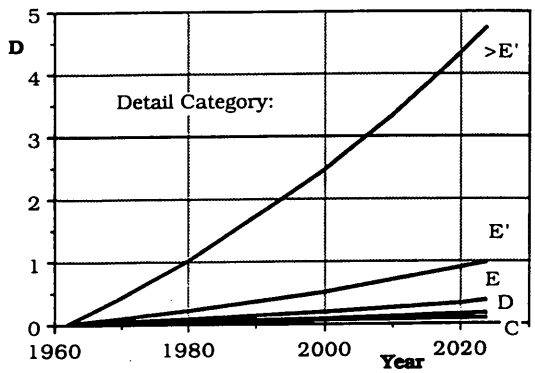

FIGURE 9 Fatigue damage estimate for girder.

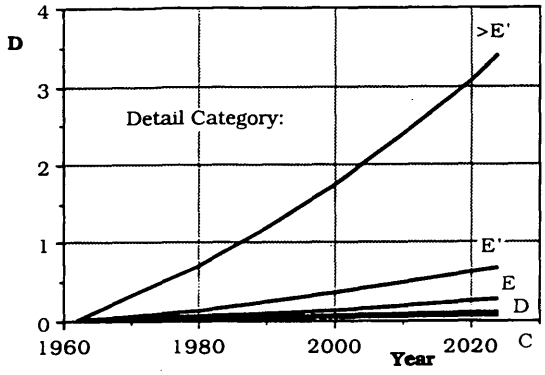

FIGURE 10 Fatigue damage estimate for floor beam.

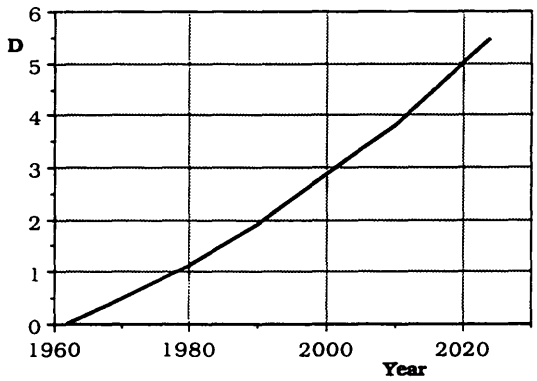

FIGURE 11 Fatigue damage estimate for stiffener intersection.

for fatigue cracking during the next 30 years of service. The girders have only Category C and D details. The floor beams have welded stiffeners, which are Category C details. The analysis indicates that no cracking is expected at these welded details on either the girders or floor beams.

CONCLUSIONS

A procedure is presented for evaluation of fatigue performance of an existing steel girder bridge. The study is focused on the development of fatigue load spectra. The structure is instrumented and truck loads are recorded. A control truck is used to verify load distribution factors. Stress history was measured under normal traffic conditions. The fatigue performance is evaluated by comparison of load (number of cycles and effective stress range) and fatigue strength.

The proposed procedure is demonstrated on a fatigue performance evaluation of an actual bridge. Based on this study, it was found that the main girder flanges should not exhibit fatigue cracking at the flange butt welds and stiffener welds during the next 30 years of service. Cracking in the webs of the girder and in the floor beams caused by the restraint of the connection between the floor beam and the girder may occur. It may also occur in the girder webs at the stiffener intersections. These web cracks are slow-growing cracks that may be detected and repaired easily. This should be considered a maintenance problem and not a safety tissue.

Based on the available information, measurements, and analysis, it is found that the bridge evaluated is capable of continued service for an unlimited period of time. The measured fatigue load spectra are within the stress ranges for unlimited periods. However further fatigue cracks may be expected in fatigue-prone details at the end of the floor beams and possibly at the longitudinal-to-transverse stiffener intersections. In the future more refined analysis and field studies are needed to determine the extent of the possible cracking and development of required retrofits. Inspection of these suspect areas should be undertaken regularly.

Previously observed cracks in transverse beams are caused by the differences in girder stiffness between exterior and interior girders. Therefore further cracking may be expected. However these are slow-growing cracks, their potential location is known, they are accessible for inspection from the walkways, and therefore they do not pose a serious problem.

AASHTO specifications provide the requirements and provisions for analytical evaluation of fatigue performance for bridge components. The tests demonstrated that experimental results can provide additional information about the actual load distribution and fatigue load spectra for components and details. This can improve the accuracy of fatigue life predictions.

ACKNOWLEDGMENTS

The study was performed for the Maryland Office of FHWA. Maryland DOT supported the field work and traffic count. Thanks are due to Tadeusz Alberski for his help in the instrumentation and measurements.

REFERENCES

1. K. H. Frank and A. S. Nowak. *Report on Evaluation of Remaining Life in Structural Steel Portion of Approach Spans of Woodrow Wilson Bridge Carrying I-95 over the Potomac River*. FHWA, U.S. Department of Transportation, Baltimore, Md., May 1991.
2. K. H. Frank. Using Measured Stress Histories to Evaluate the Remaining Fatigue Life of Bridges. In *Bridge Rehabilitation* (Konig and Nowak, eds.), Ernst & Sohn, Berlin, Germany, 1992.
3. F. J. Zwerneman and K. H. Frank. Fatigue Damage Under Variable Amplitude Loads. *Journal of Structural Engineering*, Vol. 114, No. 1, 1988, pp. 76–83.

Publication of this paper sponsored by Committee on Dynamics and Field Testing of Bridges.